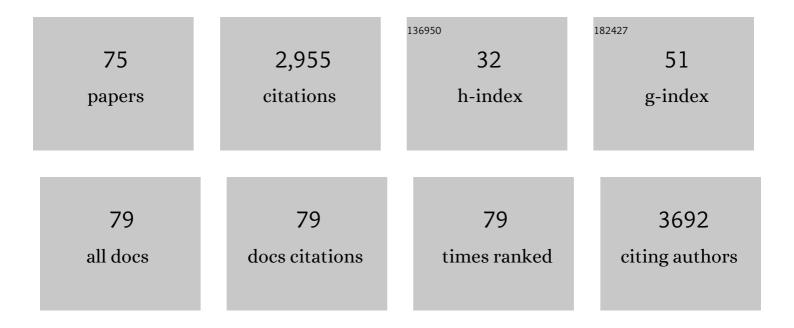
## Tao He

## List of Publications by Year in descending order

Source: https://exaly.com/author-pdf/639364/publications.pdf Version: 2024-02-01



TAO HE

#	Article	IF	CITATIONS
1	Terahertz Detectors Based on Carbon Nanomaterials. Advanced Functional Materials, 2022, 32, 2107499.	14.9	19
2	Terahertz Metamaterial Absorbers. Advanced Materials Technologies, 2022, 7, .	5.8	27
3	Metamaterialsâ€Based Photoelectric Conversion: From Microwave to Optical Range. Laser and Photonics Reviews, 2022, 16, .	8.7	11
4	Photocatalytic materials applications for sustainable agriculture. Progress in Materials Science, 2022, 130, 100965.	32.8	10
5	Recent advances in and comprehensive consideration of the oxidation half reaction in photocatalytic CO <sub>2</sub> conversion. Journal of Materials Chemistry A, 2021, 9, 87-110.	10.3	30
6	Study on nanoporous CuBi2O4 photocathode coated with TiO2 overlayer for photoelectrochemical CO2 reduction. Chemosphere, 2021, 264, 128508.	8.2	24
7	Facile modulation of different vacancies in ZnS nanoplates for efficient solar fuel production. Journal of Materials Chemistry A, 2021, 9, 7977-7990.	10.3	21
8	Water–Gas Shift Reaction on Titania-Supported Single-Metal-Atom Catalysts: The Role of Cation (Ti) and Oxygen Vacancy. Journal of Physical Chemistry C, 2021, 125, 8620-8629.	3.1	12
9	ZnSe/CdSe Z-scheme composites with Se vacancy for efficient photocatalytic CO2 reduction. Applied Catalysis B: Environmental, 2021, 286, 119887.	20.2	74
10	Role of TiO <sub>2</sub> coating layer on the performance of Cu <sub>2</sub> O photocathode in photoelectrochemical CO <sub>2</sub> reduction. Nanotechnology, 2021, 32, 395707.	2.6	7
11	Hybrid Density Functional Theory Study on Structural and Optoelectronic Properties of ZnSe <sub>1–<i>x</i></sub> Te <sub><i>x</i></sub> for the Photocatalytic Applications. Journal of Physical Chemistry C, 2021, 125, 16235-16245.	3.1	13
12	Efficient reduction of CO2 to CO over grain boundary rich gold film reconstructed by O2 plasma treatment. Applied Catalysis A: General, 2021, 625, 118333.	4.3	6
13	Recent advances in zinc chalcogenide-based nanocatalysts for photocatalytic reduction of CO <sub>2</sub> . Journal of Materials Chemistry A, 2021, 9, 23364-23381.	10.3	25
14	Ar-plasma activated Au film with under-coordinated facet for enhanced and sustainable CO2 reduction to CO. Journal of CO2 Utilization, 2021, 54, 101776.	6.8	9
15	Enhancing TiO2 activity for CO2 photoreduction through MgO decoration. Journal of CO2 Utilization, 2020, 35, 106-114.	6.8	43
16	Electrochemical reduction of CO <sub>2</sub> : Two―or threeâ€electrode configuration. International Journal of Energy Research, 2020, 44, 548-559.	4.5	13
17	Boosting visible-light driven solar-fuel production over g-C3N4/tetra(4-carboxyphenyl)porphyrin iron(III) chloride hybrid photocatalyst via incorporation with carbon dots. Applied Catalysis B: Environmental, 2020, 265, 118595.	20.2	31
18	New aspects of C2 selectivity in electrochemical CO <sub>2</sub> reduction over oxide-derived copper. Physical Chemistry Chemical Physics, 2020, 22, 2046-2053.	2.8	35

#	Article	IF	CITATIONS
19	Solar-heating boosted catalytic reduction of CO2 under full-solar spectrum. Chinese Journal of Catalysis, 2020, 41, 131-139.	14.0	58
20	Composition-tunable ZnS1–Se nanobelt solid solutions for efficient solar-fuel production. Chinese Journal of Catalysis, 2020, 41, 1663-1673.	14.0	6
21	Crystal Facet-Dependent CO <sub>2</sub> Photoreduction over Porous ZnO Nanocatalysts. ACS Applied Materials & Interfaces, 2020, 12, 56039-56048.	8.0	52
22	Unraveling the selectivity puzzle of H2 evolution over CO2 photoreduction using ZnS nanocatalysts with phase junction. Applied Catalysis B: Environmental, 2020, 274, 119115.	20.2	23
23	Visible and near-infrared dual-band photodetector based on gold–silicon metamaterial. Applied Physics Letters, 2020, 116, .	3.3	10
24	First-principles calculations of wurtzite ZnS1-xSex solid solutions for photocatalysis. Materials Today Communications, 2019, 21, 100672.	1.9	10
25	Computational study on interactions between CO2 and (TiO2) <i>n</i> clusters at specific sites. Chinese Journal of Chemical Physics, 2019, 32, 674-686.	1.3	29
26	Low-epsilon titanium oxide antenna infrared photodetector. Optics Express, 2019, 27, 5280.	3.4	1
27	Optimization of charge behavior in nanoporous CuBi2O4 photocathode for photoelectrochemical reduction of CO2. Catalysis Today, 2019, 335, 388-394.	4.4	38
28	ZnTe-based nanocatalysts for CO2 reduction. Current Opinion in Green and Sustainable Chemistry, 2019, 16, 7-12.	5.9	18
29	A computational study on linear and bent adsorption of CO2 on different surfaces for its photoreduction. Catalysis Today, 2019, 335, 278-285.	4.4	13
30	Influence of defects in porous ZnO nanoplates on CO2 photoreduction. Catalysis Today, 2019, 335, 300-305.	4.4	38
31	Cu2O-tipped ZnO nanorods with enhanced photoelectrochemical performance for CO2 photoreduction. Applied Surface Science, 2018, 443, 209-216.	6.1	46
32	Synergistic Effect of Charge Generation and Separation in Epitaxially Grown BiOCl/Bi <sub>2</sub> S <sub>3</sub> Nano-Heterostructure. ACS Applied Materials & Interfaces, 2018, 10, 15304-15313.	8.0	95
33	Interfacial charge kinetics of ZnO/ZnTe heterostructured nanorod arrays for CO 2 photoreduction. Electrochimica Acta, 2018, 272, 203-211.	5.2	15
34	Highly efficient visible-light driven photocatalytic reduction of CO2 over g-C3N4 nanosheets/tetra(4-carboxyphenyl)porphyrin iron(III) chloride heterogeneous catalysts. Applied Catalysis B: Environmental, 2018, 221, 312-319.	20.2	186
35	Modification of Ag nanoparticles on the surface of SrTiO3 particles and resultant influence on photoreduction of CO2. Applied Surface Science, 2018, 434, 717-724.	6.1	36
36	Visible-light-driven CO <sub>2</sub> photoreduction over Zn <sub>x</sub> Cd <sub>1â^`x</sub> S solid solution coupling with tetra(4-carboxyphenyl)porphyrin iron( <scp>iii</scp> ) chloride. Physical Chemistry Chemical Physics, 2018, 20, 16985-16991.	2.8	25

#	Article	IF	CITATIONS
37	Common-cation based Z-scheme ZnS@ZnO core-shell nanostructure for efficient solar-fuel production. Applied Catalysis B: Environmental, 2018, 238, 518-524.	20.2	55
38	Revisiting Electrochemical Reduction of CO <sub>2</sub> on Cu Electrode: Where Do We Stand about the Intermediates?. Journal of Physical Chemistry C, 2018, 122, 18528-18536.	3.1	32
39	Highly efficient visible-light driven solar-fuel production over tetra(4-carboxyphenyl)porphyrin iron(III) chloride using CdS/Bi2S3 heterostructure as photosensitizer. Applied Catalysis B: Environmental, 2018, 238, 656-663.	20.2	80
40	Ethylenediamine-functionalized CdS/tetra(4-carboxyphenyl)porphyrin iron(III) chloride hybrid system for enhanced CO2 photoreduction. Applied Surface Science, 2018, 459, 292-299.	6.1	22
41	Modulation of oxygen vacancy in hydrangea-like ceria via Zr doping for CO2 photoreduction. Applied Surface Science, 2018, 452, 498-506.	6.1	25
42	Visibleâ€Light Photoreduction of CO <sub>2</sub> to CH <sub>4</sub> over ZnTeâ€Modified TiO <sub>2</sub> Coralâ€Like Nanostructures. ChemPhysChem, 2017, 18, 3203-3210.	2.1	13
43	An electrochemiluminescent biosensor for dopamine detection using a poly(luminol–benzidine) Tj ETQq1 1 0.2	784314 rg 2.8	BT <sub>3</sub> Overloc
44	Facile synthesis of Bi 2 S 3 nanoribbons for photocatalytic reduction of CO 2 into CH 3 OH. Applied Surface Science, 2017, 394, 364-370.	6.1	101
45	Controllable Modulation of Morphology and Photocatalytic Performance of ZnO Nanomaterials <i>via</i> pH Adjustment. Wuli Huaxue Xuebao/ Acta Physico - Chimica Sinica, 2016, 32, 543-550.	4.9	5
46	Photocatalytic Reduction of CO <sub>2</sub> over Heterostructure Semiconductors into Valueâ€Added Chemicals. Chemical Record, 2016, 16, 1918-1933.	5.8	58
47	Preparation of CdS@CeO2 core/shell composite for photocatalytic reduction of CO2 under visible-light irradiation. Applied Surface Science, 2016, 390, 550-559.	6.1	96
48	Simple colorimetric detection of dopamine using modified silver nanoparticles. Science China Chemistry, 2016, 59, 387-393.	8.2	24
49	Synthesis and characterization of polyaniline/Zr-Co-substituted nickel ferrite (NiFe <sub>1.2</sub> Zr <sub>0.4</sub> Co <sub>0.4</sub> O <sub>4</sub> ) nanocomposites: their application for the photodegradation of methylene blue. Desalination and Water Treatment, 2016, 57, 12168-12177.	1.0	4
50	Influence of monomer concentration during polymerization on performance and catalytic mechanism of resultant poly(3,4-ethylenedioxythiophene) counter electrodes for dye-sensitized solar cells. Electrochimica Acta, 2015, 173, 796-803.	5.2	23
51	Hollow and mesoporous ZnTe microspheres: synthesis and visible-light photocatalytic reduction of carbon dioxide into methane. RSC Advances, 2015, 5, 6186-6194.	3.6	48
52	Fast, sensitive and selective colorimetric gold bioassay for dopamine detection. Journal of Materials Chemistry B, 2015, 3, 6019-6025.	5.8	29
53	Preparation of 2D hydroxyl-rich carbon nitride nanosheets for photocatalytic reduction of CO <sub>2</sub> . RSC Advances, 2015, 5, 33254-33261.	3.6	109
54	Photoreduction of carbon dioxide using strontium zirconate nanoparticles. Science China Materials, 2015, 58, 634-639.	6.3	12

#	Article	IF	CITATIONS
55	Synthesis of a Bi <sub>2</sub> S <sub>3</sub> /CeO <sub>2</sub> nanocatalyst and its visible light-driven conversion of CO <sub>2</sub> into CH <sub>3</sub> OH and CH <sub>4</sub> . Catalysis Science and Technology, 2015, 5, 5208-5215.	4.1	55
56	Design of a sector bowtie nano-rectenna for optical power and infrared detection. Frontiers of Physics, 2015, 10, 1.	5.0	16
57	Preparation of thickness-tunable BiOCl nanosheets with high photocatalytic activity for photoreduction of CO <sub>2</sub> . RSC Advances, 2015, 5, 100244-100250.	3.6	62
58	Synthesis of Cr-doped SrTiO3 photocatalyst and its application in visible-light-driven transformation of CO2 into CH4. Journal of CO2 Utilization, 2015, 12, 43-48.	6.8	85
59	Preparation of polypyrrole thin film counter electrode with pre-stored iodine and resultant influence on its performance. Journal of Power Sources, 2015, 274, 1076-1084.	7.8	21
60	Visibleâ€Light Photocatalytic Conversion of Carbon Dioxide into Methane Using Cu <sub>2</sub> O/TiO <sub>2</sub> Hollow Nanospheres. Chinese Journal of Chemistry, 2015, 33, 112-118.	4.9	47
61	Formation of Highly Stable Self-Assembled Alkyl Phosphonic Acid Monolayers for the Functionalization of Titanium Surfaces and Protein Patterning. Langmuir, 2015, 31, 140-148.	3.5	15
62	In situ synthesis of ZnO/ZnTe common cation heterostructure and its visible-light photocatalytic reduction of CO2 into CH4. Applied Catalysis B: Environmental, 2015, 166-167, 345-352.	20.2	110
63	Preparation and characterization of SrTiO <sub>3</sub> –ZnTe nanocomposites for the visible-light photoconversion of carbon dioxide to methane. RSC Advances, 2014, 4, 48411-48418.	3.6	50
64	Controlled morphology modulation of anodic TiO2 nanotubes via changing the composition of organic electrolytes. Physical Chemistry Chemical Physics, 2014, 16, 11502.	2.8	7
65	Self-Assembled CoS <sub>2</sub> Nanocrystal Film as an Efficient Counter Electrode for Dye-Sensitized Solar Cells. Journal of Physical Chemistry C, 2014, 118, 24877-24883.	3.1	69
66	Influence of doping anions on structure and properties of electro-polymerized polypyrrole counter electrodes for use in dye-sensitized solar cells. Journal of Power Sources, 2014, 246, 491-498.	7.8	50
67	High-performance polyaniline counter electrode electropolymerized in presence of sodium dodecyl sulfate for dye-sensitized solar cells. Journal of Power Sources, 2014, 253, 300-304.	7.8	61
68	The working mechanism and performance of polypyrrole as a counter electrode for dye-sensitized solar cells. Journal of Materials Chemistry A, 2014, 2, 12805-12811.	10.3	26
69	The doping mechanism of Cr into TiO2 and its influence on the photocatalytic performance. Physical Chemistry Chemical Physics, 2013, 15, 20037.	2.8	99
70	Study of H2SO4 concentration on properties of H2SO4 doped polyaniline counter electrodes for dye-sensitized solar cells. Journal of Power Sources, 2013, 242, 438-446.	7.8	46
71	Preparation and photolithography of self-assembled monolayers of 10-mercaptodecanylphosphonic acid on glass mediated by zirconium for protein patterning. Colloids and Surfaces B: Biointerfaces, 2013, 108, 66-71.	5.0	14
72	Synthesis of Indium Borate and Its Application in Photodegradation of 4-Chlorophenol. Environmental Science & Technology, 2012, 46, 2330-2336.	10.0	69

#	Article	IF	CITATIONS
73	Low temperature fabrication of ZnO compact layer for high performance plastic dye-sensitized ZnO solar cells. Electrochimica Acta, 2012, 69, 97-101.	5.2	28
74	Facile synthesis of ZnO nanocrystals via a solid state reaction for high performance plastic dye-sensitized solar cells. Nano Research, 2012, 5, 1-10.	10.4	42
75	Improved visible light photocatalytic activity of titania doped with tin and nitrogen. Journal of Materials Chemistry, 2011, 21, 144-150.	6.7	106